Multi-Scale Numerical Simulation of Tsunami-Driven Debris-Field Impacts

Justin Bonus[a], Pedro Arduino[b], Michael Motley[c], Marc Eberhard[d]
University of Washington, Seattle, USA
[a]bonusj@uw.edu, [b]parduino@uw.edu, [c]mrmotley@uw.edu, [d]eberhard@uw.edu

Abstract. In current practice, debris-field impact loading for near-water structures is usually derived from (i) infrequent case histories, (ii) simplified analytical equations, and (iii) practitioner experience. Via advanced numerical simulation of tsunami-driven debris-field impacts at multiple scales and conditions, we are now forging a modeling approach to address a wider range of scenarios. Broadened cases are characterized, with chaotic natures expressed stochastically. The analytical tools have the potential to strengthen the basis of ASCE-7 guidelines and to encompass events not yet described in the code.

Introduction

Coastal infrastructure is vulnerable to the barely quantified hazard of debris-field impacts and damming during inundation events. Faced with potentially significant design consequences, engineers find themselves lightly equipped. Debris-fields are mobilized groups of debris (e.g. cars, logs, cargo crates) that may collide with structures. Resultant loads are chaotic (i.e. hard to predict) even when composing debris are known. Notoriously difficult to record in nature, recreate in experiments, and simulate in software, debris-field design is in its infancy. Our group is tackling the problem via a three-point approach: (i) multi-scale experiments, (ii) multi-scale numerical simulations, and (iii) a boiled-down probabilistic framework of design.

Hundreds of experiments, executed at two wave flumes of vastly different scales (10m and 100m length), create a data-set of varied tsunami-driven debris-field impacts. Behavior is studied respective to facilities, fluid conditions, and debris-field configurations.

Inspired by animation studios like Disney, we advance debris-field hazard modeling with a powerful numerical tool. Experimental facilities the length of football fields are measured to the inch and filled by 50 million+ numerical bodies– Greater than the combined population of Washington, Oregon, and California. 6 million+ time-steps are executed. A person walking each could travel from Los Angeles to Honolulu. Graphics processing units (GPUs), often used for video-games, accelerate our hazard simulations via massive parallelism, bringing simulations times from days to hours. We achieve staggering fidelity not previously possible for tsunami-driven debris-field simulations.

Informed by experimental and numerical results, we take initial steps into a performance-based engineering framework of design for tsunami-driven debris-field hazards where a new characterization scheme is proposed. Limitations and lines of future research are discussed.

Debris-Fields

ASCE 7-16 and FEMA P-646 suggest limited design guidelines, only applicable to basic single-debris scenarios. Though consistent with the best available science, debris-field loading has been identified as a subject for improvement in the upcoming ASCE 7-22 revision [1]. This paper documents our effort to advance understanding of stochastic debris-field loading, but many challenges are faced.

Current design guidelines prioritize single-debris impacts. Stiffness and velocity control load predictions via simple equations [20]. They assume elastic collision of debris characterized as a 1D bar

with full momentum transfer. Stiffness of debris (k), impact duration (t), and max force of impact (**f**) are found as:

$$k = \frac{EA}{L} \quad \text{and} \quad t = 2\sqrt{\frac{m}{k}} \quad \text{and} \quad \mathbf{f} = v\sqrt{mk} \tag{1}$$

Where E is the debris' Young's modulus, A is area of impact, L is length of debris, v is velocity of impact, and m is mass of debris. Complex debris require more information, but one may phrase basic debris design parameters as set $\mathbb{D}$:

$$\mathbb{D} = \{\rho, E, A, L\} \tag{2}$$

This quantifies common debris hazards, but it does not capture debris-fields, complex debris, fluid conditions, or obliquity of impact. Proposed methods account for obliquity, water displacement, drag, and mobilization, however, no current approach extrapolates into debris-field hazards.

Debris-field hazards are short-duration, infrequent, and highly variant. Data is perishable from inundation drawback and post-disaster clean-up [3] so little is known about them. Further, loads are chaotic and so require large volumes of nonexistent observations to characterize stochastically. Empirical frameworks negated by minimal records, simulations opposed by computational and hazard complexity, and theory subverted by dynamic, nonlinear debris-fluid-structure interaction (DFSI), this document is a window into our active remedy.

Experiments

A sister-piece submitted at this conference ("Quantifying and Understanding Structural Loading from Wave-Driven Debris Fields") and a planned publication finely detail our tsunami-driven debris-field experiments. Here, dual wave flume tests are briefly summarized before leading into our numerical simulations, which recreate these experiments, and proposed framework, which builds on top of experimental observations.

We executed hundreds of fluid-driven debris-field hazards experiments, covering a swath of debris configuration and fluid events. Performed at two wave flumes of vastly different scales (UW WASRIF and OSU LWF, 10m vs. 100m length) our tests **(i)** observe scale-effects, **(ii)** test different fluid-flow conditions, and **(iii)** reduce bias towards facility details.

Both flumes use an aluminum structural box to represent a scaled building. They are equipped with load-cells and pressure sensors to measure structural demands. Water velocity and depth is measured at key locations in the flumes. Various sizes of High Density Poly Ethylene (HDPE, buoyant on water) debris are placed in ordered and random configurations to create debris-fields. Collisions of debris-fields with the structures are recorded by load-cells for comparison of debris-fields and structural demands.

Small-scale testing was performed at the Univeristy of Washington's (UW) Washington Air-Sea Interaction Research Facility (WASIRF) (Fig. 1). Near steady-state flow is reached for many pairing of flow-velocity and flow-depth. At this small-scale, results have been limited. Notably, debris impacts are difficult to resolve relative to hydrodynamic loads. Experiments were executed in August 2021. Our group intends to revisit this facility in 2022.

Large-scale testing was performed at Oregon State University's (OSU) Large Wave Flume (LWF) (Fig. 1), a facility for two-dimensional characterization of ocean-shore wave advancement [11]. Breaking and non-breaking solitary waves are studied as they progress up a series of ramps, representing the shore, before impacting a scaled structure. Previous debris-field studies by our group were performed here in 2017 [2]. Our most recent study was in Spring of 2021 and has shown promising results for

Fig. 1: Wave flume facilities where tsunami-driven debris-field tests were executed. (Left) UW WASIRF. (Right) OSU LWF.

resolving structural demand trends with not just debris count, but also refined statistical aspects of debris-field configurations (e.g. ”density” and orientation).

A primary lesson learned was the inadequacy of the smaller flume (UW WASIRF). Scale effects caused the debris impact and damming loads to be poorly observed. Buffers of water formed at points of impact which debris were not heavy enough to displace. Debris slowed in front of the structures as a result, often lightly impacting or missing completely. The larger flume (OSU LWF) did resolve debris and debris-field impacts respective to not only the number of debris but also their geometric configuration (e.g. ”density” and orientation), showing a hazard unique to debris-fields. This demonstrates the importance of scale in tsunami-driven debris-field experiments. We believe some phenomena are still being missed at even the OSU LWF, which is the length of a football field and outside the budget of many groups. Further hazard aspects might only be seen at true scale but this is prohibitively expensive to recreate. Simulations that can digitally recreate our scaled tests and then extrapolate to real sizes may be the solution.

Simulations

Tsunamis, landslides, and avalanches driving debris-fields are computationally complex coinciding hazards. Yet, in recent 3D animated films these events are rendered to an incredible visual benchmark at computational scale exceeding what most engineers can match. Modern animators employ engineering techniques, i.e. physics-based animation, to achieve renders that align with real world behavior. Disney’s Frozen, in an effort to simulate snow media (history-dependent, topology changing, large-deformation, and nonlinear), champions an interesting but expensive numerical tool: The Material Point method (MPM). Their software optimization bypassed a computational barrier that had limited engineering use. Just as animators adopt engineering techniques to improve physical accuracy, we argue engineers should adopt the optimized codes of computer graphics professionals. Doing so can accelerate engineering simulations 10x - 100x, and grow them by 2x - 10x. We achieve this with minimal overhead in our own project.

Project schedules have tasks done in parallel, numerical methods allow the same. Graphics processing units (GPUs) possess thousands of computational cores that run independently. Typically used by video-games to execute photo-realistic physics and lighting 60+ times per second, GPUs can accelerate engineering physics software by 100x. Multiple GPUs scale this effect. Still, programming for GPUs is a learning curve that few engineers have the time to surmount. By retooling (i.e. modify for engineer use) and validating (i.e. show results are physically accurate), extraordinarily fast animation

software can be leveraged by engineers with little GPU expertise at low-overhead. Code used in our project is based on a open-source, Multi-GPU, optimized MPM software (Claymore, [10]) developed for animation purposes, now modified to engineering standards.

The Material Point Method (MPM) is a numerical tool suited to large-deformation mechanics (e.g. tsunamis, landslides), multi-phase multi-material interaction (e.g. debris-fluid-structure interaction), history-dependent materials (e.g. soft-body cars, concrete, mud), and topology change (e.g. fracturing, erosion). It is easy to use, as no meshes are required and a uniform background grid applies boundary conditions. An ideal candidate for tsunami-driven debris-field impacts, use is only limited by massive computational requirements. Multi-GPU implementations offer the solution.

Here we develop a modelling approach to tackle fluid-driven debris-field hazards. Our numerical tool, a multi-physics coupling of the material point method (MPM) [14] and finite elements (FEM), scales across Multi-GPUs in high-performance computing centers (HPCs), diluting computational weight. Prioritizing flexibility, speed, and simplicity leads to the most basic algorithm approach for DFSI identified yet. A shortlist of problem requirements and our approach's answers are:

1. **Multi-Material and Multi-Phase Interaction.** MPM does this without any user effort. It solves the equation of motion (EOM) on a shared background grid but the material models on independent particles [14], passing results back-and-forth per time-step to achieve collision consensus. Most methods struggle in this key requirement, such as finite element analysis (FEA), smoothed particle hydrodynamics (SPH) [22], and computational fluid dynamics (CFD).

2. **Large-Deformations Dynamics.** Needed for debris transport and complex materials. MPM is well-suited [14] due to its "resetting" grid for the EOM. This avoids mesh tangling found in FEA.

3. **Contact Mechanics.** Neccesary for DFSI, MPM has natural contact between all materials. However, it is at grid-cell resolution (gaps of Δx at contact) and undesirably "sticky" (water may latch onto debris). Sub-grid resolution (minimal gap) and "slip" contact (debris slides on water) is needed. We vet the Affine-Separable Fluid-Implicit-Particle method (ASFLIP) [8], a computer graphics innovation. With roots in FLIP [17] and APIC [4], ASFLIP break "sticky" contact selectively. Particle velocity is saved across time-steps, being used in both the position and velocity update (similar to PIC/FLIP mixing [16]) to correct contact strongly local to tension (e.g. surfaces pull-apart) and not at all for compression (e.g. collision, buoyancy). Not as theoretically founded as advanced nonlinear contact models, ASFLIP use is easy and fast while producing reasonable contact if tuned well, earning our recommendation.

4. **Material Models.** MPM supports nearly any material with ease. For water we use a weakly-compressible fluid model [18], Murnaghan-Tait equation of state plus a small viscous stress. Imcompressible models were considered [9] [7] but simplicity is preferred for Multi-GPU implementation. For debris (HDPE plastic in experiments) we use the Fixed-Corotated model (large-deformation, hyper-elastic). Also available are Modified Non-Associative Cam-Clay and Drucker-Prager models, which are not yet fully vetted in the software.

5. **Damping and Noise Mitigation.** MPM is not favorable as both can grow large. High particle-per-cell values (PPC, average particle count contributing to a grid-node) reduce degrees-of-freedom (DOF) during P2G [15] and causes errors, namely for stiff material. Computational costs constrain grid resolution and thereby physical behavior on a length basis (e.g. damps small vortexes in water). Our approach is two-part. Firstly, PPC is kept low (2.5 to 8) to reduce transfer

Table 1: Numerical Implementation Specification Sheet

Parameter	Specification
Method	Material Point Method (MPM)
Time Integration	Explicit
Grid	Uniform Cartesian
Transfer-Scheme	APIC, MLS-MPM
Advection-Scheme	PIC/FLIP, ASFLIP
Shape-Functions	Quadratic B-Splines
Contact Algorithm	ASFLIP and FEM coupling
FEM Formulation	Large-Deformation, Total Lagrangian
FEM Elements	Linear Tetrahedrons
Debris Model	Fixed-Corotated Solid
Water Model	Weakly-Compressible Fluid
Systems	TACC Frontera, Hyak Klone, Laptop
Accelerators	NVIDIA Quadro 5000, 2080 ti, 1060m

errors while grid-node count is increased by orders of magnitude using Multi-GPU acceleration, i.e. brute-forcing physical resolution. Secondly, treating angular velocity via the Affine Particle-in-Cell method (APIC) [4], developed by computer graphics researchers. A small change in G2P to improve P2G angular momentum contribution, APIC minimizes MPM's rotational damping and is easy to implement (a few lines of code). Debris transport on water and basic fluid turbulence is notably improved. For further angular refinement (e.g. sub-grid turbulence) refer to PolyPIC [24], a higher-order APIC. Traditional filtering schemes [6] [15] [19] improve MPM noise but can be too specific and complex. We broadly recommend minimizing PPC and implementing expanded transfer-schemes (APIC) to counter damping and noise with low-overhead.

6. **Timely Execution.** Computation cost insofar is extreme in serial codes, but a massively parallel version remedies this. Adopting optimized computer graphics software that scales on Multi-GPUs accelerates this engineering approach roughly 100x over CPU codes. We strongly recommend high-performance implementations, namely Multi-GPU, to fully leverage MPM– Bringing simulation times from days to hours.

Finite Elements are incorporated to leverage the breadth of FEA literature. We apply a total Lagrangian scheme [21] [23] for large deformations. Elements are linear tetrahedrons. Vertices are MPM particles that receive velocity from the MPM grid. Deformation and stress relative to advected vertices is then computed at element single-Gauss points (i.e. element center)– not the MPM points. Internal forces map from elements to vertices. Vertices then map internal forces and momentum to the MPM grid and the process repeats. Coupling is as basic as possible, despite how it may sound. Groups of FE debris can now separate and interact using a basic contact algorithm (ASFLIP) even if tightly packed (unlike standalone MPM) and individual debris do not spuriously break apart. More complex debris (e.g. concrete masses, logs) may desire topology change (e.g. cracking, splintering) which is achievable by standard MPM or FEM variants. We recommend our reduced MPM-FEM coupling unless further needs exist.

Validation of debris-fluid-structure interaction (DFSI) requires **(i)** debris-structure interaction (DSI), **(ii)** debris-fluid interaction (DFI), **(iii)** fluid-structure interaction (FSI), and **(iv)** debris-debris interaction (DDI). Respectively, we evaluated the code for: **(i)** in-air elastic debris impact case where forces

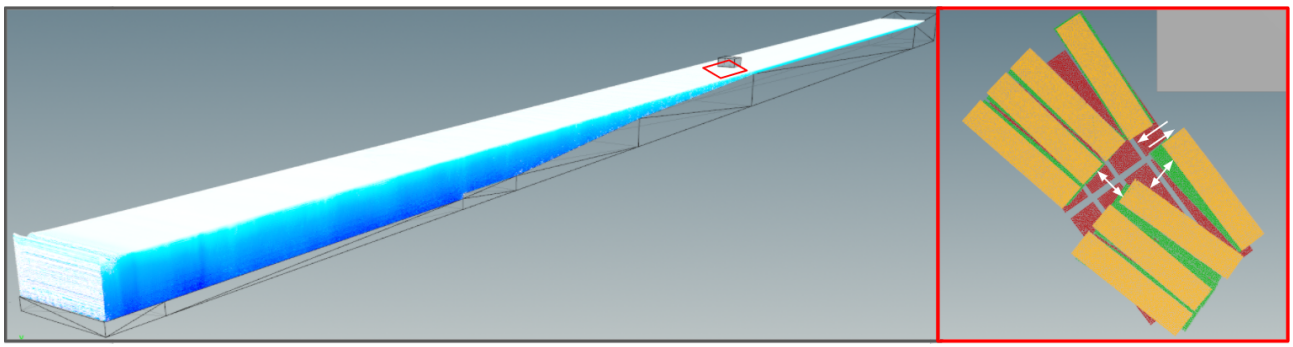

Fig. 2: (Left) Simulation of OSU LWF. 50 million+ water particles. Grid-cells of 1”. Pressure visualized in fluid. Wireframe base represents the bathymetry ramps at the OSU LWF. Grey box is the scaled structure. Water disturbance on tfar-left is from the wave-maker piston beginning to move. Red square at upper-right is domain of the adjacent figure. (Right) Plan-view of debris-fields before impact with grey structure. Red debris is regular MPM. Green debris is MPM+ASFLIP. Yellow debris is MPM+ASFLIP+FEM. Respectively, debris-debris interaction is poor, decent, and good. Different color debris are in different simulations.

on a structure are measured and compared to analytical equations (Eq. 1), **(ii)** wedge displacing fluid case where proper surface contact, non-penetration, and fluid non-plasticity are checked, **(iii)** elastic flap impacted by dam break case where flap tip displacement is tracked, and **(iv)** tightly packed debris checked for allowing separation and collision. DSI results are comparable to analytical and FEM solutions. DFI shows a marked improvement over standard MPM and resolves sub-grid contact. FSI validation is within bounds produced by PFE, FEM, and an inhouse software called FOAMySees. DDI substantially improves over standard MPM with both ASFLIP and FEM coupling (Fig. 2). Confident in basic behavior, we are now validating DFSI against our experiments.

OSU experiments were recreated numerically in our code (Fig. 2). Particle counts reach as high as 50 million+ and grid-cells are as small as 1” in length. Simulations cover 40 real-world seconds and execute over 1 to 12 hours. Three GPUs model the water, while one GPU is reserved for the debris-field. Initial conditions placed water at-rest via the recorded standing water level (SWL) from experiments. Debris-fields initialized on the water-surface in designated configurations two meters from the structural box. No modifications were made for methods of placing debris from the experiments. Flume walls are modeled as rigid boundary conditions with separable velocity contact. Flume bathymetry (i.e. ramps) was recreated on the grid with a decay layer [19] applied to prevent ”stair-stepping” effects of tilted surfaces in MPM. The wave-maker is a velocity boundary condition on the grid that moves according to experimental motions of the wave-maker. Wave-gauges are placed throughout the flume to record the elevation and velocity of the wave, matching the experiments. Early results are promising, with both the numerical wave-gauges and load-cells replicating experimental readings reasonably well. However, breaking-wave cases (i.e. large waves that fold-over) show break locations that are further in the flume than experiments, suggesting breaking-wave dynamics can still be refined in our approach. Unbroken-wave cases behave well but require high-resolution to model the small 20cm wave in a 100m long flume. OSU LWF debris-field behavior is substantially improved by our coupled MPM+ASFLIP+FEM approach.

WASIRF experiments were recreated numerically. Particle counts reach as high as 6 million+ and grid-cells are as small as 5mm in length. Simulations cover 20 real-world seconds and execute over 20 minutes to 3 hours. One GPU models the water and another GPU the debris-field. Initial conditions placed water with initial stream-wise velocity and height (average of an undulating surface

elevation) from experimental readings. Debris was placed on the water surface with no initial velocity in experimental configurations. Flume walls are set as rigid, separable velocity boundaries on the grid. The facility has water pumped inflows and outflows at either end of the flume but are modelled as extended run-ins and run-outs to avoid complex pressure boundary conditions. The structural box is a rigid, separable velocity boundary on the grid. Results are promising but remain preliminary, as full analysis of the experimental UW WASIRF tests is active and a facility revisit is planned.

We developed a flexible, fast, and fairly simple numerical approach for the complexities of tsunami-driven debris-fields hazards and general DFSI. Inspired by computer graphics professionals, optimized Multi-GPU codes accelerate this tool by 100x, bringing simulation times from days to hours. However, design guidelines should not rely on advanced simulations when possible. Critical quantification of fluid-driven debris-field impact hazards is to be built on foundations of our experimental and numerical trials in the following section.

Framework

Great uncertainty exists in structural design for tsunami-driven debris-field hazards. In the light of hundreds of experimental and simulated tests, the authors believe a framework for probabilistic behavior is possible. Initial steps, limitations, and insights are discussed here.

Performance Based Engineering (PBE) is a clean, probabilistic hazard workflow [12]. Our debris-field framework is an add-on to existing PBE frameworks, specifically Performance Based Tsunami Engineering (PBTE), and is coupled similar to other combined hazard studies [13]. Guided by experimental and numerical results, we take the following steps:

1. Define debris-field parameters of novel significance, $\mathbb{F}$, $p(\mathbb{F})$.
2. Declare debris-field intensity measures, IM.
3. Determine debris-field intensity measures given prior conditions, $p(IM|O, D, \mathbb{F})$.
4. Connect engineering demand parameters to debris-field intensity measures, $p(EDP|IM)$.

To start, determine the initial conditions for analysis. This includes location (O) and design (D), as standard. Establish another parameter set ($\mathbb{F}$) for the debris-field. Parameters are measures of: **(i)** count, **(ii)** obliquity, **(iii)** occupation, and **(iv)** time-dependency. These independent variables must be measurable, minimal, scale-invariant, and predictive of engineering loads (i.e. dependent variables). A set of debris-field independent variables ($\mathbb{F}$) is stated.

$$\mathbb{F} = \{\mathbb{D}, \mathbf{c}, \mathbf{n}, \boldsymbol{\theta}\} \quad \text{and} \quad p(\mathbb{F}) = \{\mathbb{F}, T\} \tag{3}$$

Where $\mathbf{c}$, $\mathbf{n}$, and $\boldsymbol{\theta}$ are placeholder measures of debris count, occupation, and orientation. $\mathbb{D}$ is inherited from current single-debris design (Eq. 2) and T is time-periods that preceding variables act respective of (e.g. daily, monthly, seasonally). Distinction of debris-fields vs. debris ($\mathbb{F}$ vs. $\mathbb{D}$) is important because unique hazard loading results from different debris-field configurations (varied $\mathbb{F}$), even for consistent debris properties ($\mathbb{D}$) (Fig. 3).

Obliquity (θ) of single-debris impacts affect structural demands, such as max force [1]. However, debris-field obliquity is a distribution ($P(\theta)$), not a single-value. Drawing from geotechnical soil sieve charts, obliquity distributions are characterized by simple meta-parameters to describe the continuous

Fig. 3: **Parking Lot Debris.** (Upper-Left) Ordered parking lot. (Upper-Right) Angled parking lot. (Lower-Left) Sparse parking lot. (Lower-Right) Parking lot evolved by 2011 Tohoku tsunami.

curve, not the discrete points. Potential obliquity measures ($\boldsymbol{\theta}$) are coefficient of uniformity (C_{u}), coefficient of curvature (C_{c}), or simply percent more oblique than a critical angle (D_θ).

$$C_{\text{u}} = \frac{D_{60}}{D_{10}} \quad \text{or} \quad C_{\text{c}} = \frac{D_{30}^2}{D_{60} D_{10}} \quad \text{where} \quad D_\theta = \text{ \% debris of obliquity } \geq \theta \tag{4}$$

Occupation of a debris-field ($\mathbf{n}$) and spatial uncertainty in the measure ($P(\mathbf{n})$) influences impact demands, i.e. for max force (less "dense" fields typically enact smaller max loads). Potential occupation measures ($\mathbf{n}$) are porosity (n), void-ratio (e), and spacing (s), where A_W is the water occupied area contained in A_T which is the total area, i.e. "foot-print", of a debris-field.

$$n = \frac{A_W}{A_T} \quad \text{or} \quad e = \frac{n}{n-1} \quad \text{or} \quad s = \text{ Avg. debris spacing.} \tag{5}$$

Note that $\mathbf{c}$, $\mathbf{n}$, and $\boldsymbol{\theta}$ for any fixed footprint (e.g. 10m x 25m) are correlated by geometric constraint (i.e. not independent). Multi-linear regression technically requires independent variables, so other regression types (e.g. RIDGE, LASSO, or Elastic Net) might be preferred for significant statistical models. Using just two variables could also be viable as a result of correlation constraining the third, greatly simplifying engineering design. In our studies we observe that $\mathbf{c}$ and either $\mathbf{n}$ or $\boldsymbol{\theta}$ is often adequate for load predictions.

At-rest debris-field measures ($\mathbb{F}_{\text{Rest}}$) are definable with a site-survey, whereas at-impact values ($\mathbb{F}$) aren't known. We claim evolution of debris-field parameters at-rest to the moment of impact is predictable. Similarly, backwards evolution may apply to post event measures ($\mathbb{F}_{\text{Post}}$) from disaster reconnaissance. Field evolution equations are not our focus, see other studies for examples [3], but relationships must exist to use prior or post information to quantify the debris-field at impact.

$$\mathbb{F} = f\left(\mathbb{F}_{\text{Rest}}, O, D\right) \quad \text{and} \quad \mathbb{F} = f\left(\mathbb{F}_{\text{Post}}, O, D\right) \tag{6}$$

Time-dependency (T) phrases debris-field intensity measure (IM) as a probability of exceedence ($p(IM)$). Engineers often design by time-ranges (e.g. 100-year tsunamis) over the worst-case scenario, which can be expensive and over-conservative. 100-year tsunami design should not assume mobilization of the worst-case debris-field, but perhaps a 1-month debris-field. 100-years vs 1-month is arbitrary, but a debris-field's design time-period should be shorter because humans actively alter debris-fields (e.g. removing parking-lots, building ports, logging forests) so a long forecast is not viable, unlike tsunami prediction.

Now determine intensity measures (IM) relative to prior conditions ($p(IM|O, D, F)$). IM for tsunami-driven debris-fields are partially shared with tsunamis (e.g. flow-velocity, flow-depth) but another measure differentiates. We postulate geometric "order" (from **n** and $\boldsymbol{\theta}$) of debris-fields as a time-dependent aspect of the hazard's IM. It is an IM unique to the debris-field, not the debris or tsunami.

Finally, recap preceding claims as axioms, which in turn give a framework to predict engineering demand parameters (EDP) from debris-field intensity measures ($p(EDP|IM)$). Axioms relate initial debris-field properties to probabilistic structural impact demands via a mix of first-principals and observations in experiments and simulations. Axioms of debris-field impacts, not damming, are stated:

1. **Debris-fields are continuous, probabilistic distributions.**. Distributions of measures ($\mathbb{F}$)– No longer a summation of discrete debris. This view assists where discrete measures (e.g. debris count c) are uncertain, fields are heterogeneous (i.e. mixed debris), and spatial variance is significant.

2. **Geometric order of debris-fields is an intensity measure.** Using "order" (from occupation and orientation) to derive demands (i.e. $p(EDP|IM)$) parses geometric hazard contribution. Perfect order means zero porosity ($n = 0$, tightly packed) and no internal obliquity ($\theta = 0$, debris aligned), the most hazardous case of impact for a fixed number of debris (c). Ordered hazard is set by $C(\mathbf{c})$, experimentally studied in our ordered debris-array impacts.

3. **Deviation from order describes impact hazard reduction.** Allows existing research on ordered debris-arrays to be applied to disordered-fields. Disorder is geometric, i.e. occupation (**n**) and orientation ($\boldsymbol{\theta}$) relative to perfect order. Worst-case is set by ordered behavior ($C(\mathbf{c})$) and reduced by equations that punish deviation ($R(\boldsymbol{\theta})$, $R(\mathbf{n})$). Intuitively, a lot sparsely occupied by cars, parked at random angles, is less impact hazardous than the same cars tightly-packed side-by-side.

4. **Debris-fields are time-dependent (hourly, daily, seasonally).** Considered for at least one parameter (e.g. occupation exceedance as $\lambda(\mathbf{n}) = f(\mathbf{n}, T)$), our intensity measure is a probability of exceedence ($p(IM)$) over periods (T). Take a near-shore parking-lot, where count (**c**) and occupation (**n**) of cars is time-dependent (e.g. more cars midday than midnight, in tourist season than not). Debris-field hazards vary predictably with time.

5. **Debris-field evolution, pre-event to impact, is definable.** Evolves at-rest debris-field measurements ($\mathbb{F}_{\text{Rest}}$) for the event ($\mathbb{F}$). A parking-lot can be initially surveyed (car count, occupation, and obliquity, i.e. semi-consistently spaced cars parked roughly parallel with lot lines) and then evolution over the distance to the structure gives the probabilistic configuration at impact ($\mathbb{F}$, $p(\mathbb{F})$).

Carrying axioms to conclusion, set a potential relationship between stochastic debris-fields and an engineering demand parameter ($\mathbf{f}_{\text{Field}}$, max impact force due to debris-field). Probability of exceedence

is available ($p(\mathbf{f}_{\text{Field}})$) for performance-based design.

$$\mathbf{f}_{\text{Field}} = f(F, ...) = C(c) \int_0^{\frac{\pi}{2}} (R(\theta)P(\theta))d\theta \int_0^1 (R(n)P(n))dn \tag{7}$$

$$p(\mathbf{f}_{\text{Field}}) = f(F, ..., T) = C(c) \int_0^{\frac{\pi}{2}} (R(\theta)P(\theta))d\theta \int_0^1 (R(n)\lambda(n))dn \tag{8}$$

These axioms can give many approaches, this is one example written analytically. Ordered-field behavior ($C(\bullet)$) and disordered-field reductions ($R(\bullet)$) can be regression models of experimental, numerical, and case-study observations. Probability distributions ($P(\bullet)$) and distributions respective to time-periods ($\lambda(\bullet)$) could be from site-surveys or set by tables for common cases (e.g. typical parking lots for commercial businesses).

This framework is effective for simulated in-air debris-field impacts and its trends are reproduced in our fluid-driven experimental trials. For a real tsunami-driven event, a coupled approach is taken with PBTE. The IM should include debris-field "order", as above, along with tsunami measures (e.g. flow-depth and flow-velocity). As flow-depth and flow-velocity influence debris-field hazards (mobilization and debris-velocity respectively), coupling is natural. Our framework geometrically quantifies debris-fields on time-ranges, but it is just a small added step in a larger PBTE endeavor.

Many critical aspects will require intensive research (experimental, numerical, and via case-studies) to flesh-out and validate for peace-of-mind in design. Still, our step-by-step approach, starting at debris-field description and ending in a probabilistic and time-dependent way to quantify a coupled hazard, shows novel promise.

Conclusions

Understanding of tsunami-driven debris-field hazards on coastal structures is advanced in this paper. Current single-debris design is first summarized and shown to be fundamentally inadequate for debris-fields. Minimal real-world observations is identified as a research bottle-neck. To fill this gap, hundreds of experiments, in two flumes of vastly different scales, are executed to quantify stochastic debris-field behavior. Growing the data-set further, we develop a massively-parallel numerical approach to replicate experiments and extrapolate to real-world events. Simulations are massive, often containing more numerical bodies than the populations of Washington, Oregon, and California combined while executing in hours. Based on our many experiments and simulations, first-steps are taken into a performance-based engineering framework for tsunami-driven debris-field hazard design.

References

[1] Nistor, I., Goseberg, N., Stolle, J. (2017). Tsunami-driven debris motion and loads: A critical review. Frontiers in Built Environment, 3, 2.

[2] Shekhar, K., Winter, A. O., Alam, M. S., Arduino, P., Miller, G. R., Motley, M. R., Eberhard, M. O., Barbosa, A. R., Lomonaco, P., Cox, D. T. (2020). Conceptual Evaluation of Tsunami Debris Field Damming and Impact Forces. Journal of Waterway, Port, Coastal, and Ocean Engineering, 146(6), 04020039.

[3] Naito, C., Cercone, C., Riggs, H. R., Cox, D. (2014). Procedure for Site Assessment of the Potential for Tsunami Debris Impact. Journal of Waterway, Port, Coastal, and Ocean Engineering, 140(2), 223–232.

[4] Jiang, C., Schroeder, C., Selle, A., Teran, J., Stomakhin, A. (2015). The affine Particle-In-Cell method. ACM Transactions on Graphics, 34(4), 1–10.

[5] Chock, G. Y. K. (2016). The ASCE 7 Tsunami Loads and Effects Design Standard for the U.S.

[6] C. Mast, P. Mackenzie-Helnwein, P. Arduino, G. Miller, and W. Shin, (2012), Mitigating kinematic locking in the Material Point Method, Journal of Computational Physics, Vol. 231, Issue 16, June 2012, pp. 5351-5373.

[7] Vittoz, L., Oger, G., de Leffe, M., le Touzé, D. (2019). Comparisons of weakly-compressible and truly incompressible approaches for viscous flow into a high-order Cartesian-grid finite volume framework. Journal of Computational Physics: X, 1, 100015.

[8] Fei, Y., Huang, L., Guo, Q., Wu, R., Gao, M. (2021). Revisiting Integration in the Material Point Method: A Scheme for Easier Separation and Less Dissipation. ACM Trans. Graph, 40, 16.

[9] Zhang, F., Zhang, X., Yim Sze, K., Lian, Y., Liu, Y. (2017). Incompressible material point method for free surface flow . Journal of Computational Physics, 330, 92–110.

[10] Wang, X., Qiu, Y., Slattery, S. R., Fang, Y., Li, M., Zhu, S.-C., Zhu, Y., Tang, M., Manocha, D., Jiang, C. (2020). Article 30.. 2020. A Massively Parallel and Scalable Multi-GPU Material Point Method. ACM Trans. Graph, 39(4), 15.

[11] Lomonaco, P., Alam, M. S., Arduino, P., Barbosa, A., Cox, D. T., Do, T., Eberhard, M., Motley, M., Shekhar, K., Tomiczek, T., Park, H., Lindt, J. W. van de, Winter, A. (2018). EXPERIMENTAL MODELING OF WAVE FORCES AND HYDRODYNAMICS ON ELEVATED COASTAL STRUCTURES SUBJECT TO WAVES, SURGE OR TSUNAMIS: THE EFFECT OF BREAKING, SHIELDING AND DEBRIS. Coastal Engineering Proceedings, 36, 53–53.

[12] Moehle, J., Deierlein, G. G. (2004). A Framework Methodology for Performance-Based Earthquake Engineering.

[13] Attary, N., van de Lindt, J. W., Barbosa, A. R., Cox, D. T., Unnikrishnan, V. U. (2019). Performance-Based Tsunami Engineering for Risk Assessment of Structures Subjected to Multi-Hazards: Tsunami following Earthquake. 25(10), 2065–2084.

[14] Sulsky, D., Chen, Z., Schreyer, H. L. (1993). A particle method for history-dependent materials. Other Information: PBD: Jun 1993.

[15] Tran, Q. A., Sołowski, W. (2019). Temporal and null-space filter for the material point method. International Journal for Numerical Methods in Engineering, 120(3), 328–360.

[16] Hammerquist, C. C., Nairn, J. A. (2017). A New Method for Material Point Method Particle Updates that Reduces Noise and Enhances Stability.

[17] Brackbill, J. U., Ruppel, H. M. (1986). FLIP: A method for adaptively zoned, particle-in-cell calculations of fluid flows in two dimensions. Journal of Computational Physics, 65(2), 314–343.

[18] Tampubolon, A. P., Teran, J., Gast, T., Klár, G., Fu, C., Jiang, C., Museth, K. (2017). Multi-species simulation of porous sand and water mixtures. ACM Trans. Graph, 36.

[19] Yang, W., Arduino, P., Miller, G.R., Mackenzie-Helnwein, P. (2018). Smoothing algorithm for stabilization of the material point method for fluid–solid interaction problems. Computer Methods in Applied Mechanics and Engineering.

[20] Piran Aghl, P., Naito, C. J., Riggs, H. R. (2014). Investigating the Effect of Nonstructural Mass on Impact Forces from Elastic Debris. Structures Congress 2014 - Proceedings of the 2014 Structures Congress, 635–644.

[21] de Vaucorbeil, A., Nguyen, V. P., Hutchinson, C. R. (2020). A Total-Lagrangian Material Point Method for solid mechanics problems involving large deformations. Computer Methods in Applied Mechanics and Engineering, 360, 112783.

[22] Hasanpour, A., Istrati, D., Buckle, I. (2021). Coupled SPH–FEM Modeling of Tsunami-Borne Large Debris Flow and Impact on Coastal Structures. Journal of Marine Science and Engineering 2021, Vol. 9, Page 1068, 9(10), 1068.

[23] Irving, G., Teran, J., Fedkiw, R. (2004). Invertible Finite Elements For Robust Simulation of Large Deformation.

[24] Fu, C., Guo, Q., Gast, T., Jiang, C., Teran, J. (2017). A polynomial particle-in-cell method. ACM Transactions on Graphics, 36 (6).